Surface & Coatings Technology 205 (2010) 1470–1474

Contents lists available at ScienceDirect

Surface & Coatings Technology

journal homepage: www.elsevier.com/locate/surfcoat

Enhanced gate-induced floating-body effect in PD SOI MOSFET under external mechanical strain

Chih-Hao Dai [a], Ting-Chang Chang [a,b,c,*], Ann-Kuo Chu [a], Yuan-Jui Kuo [a], Shih-Ching Chen [b], Chih-Tsung Tsai [b], Wen-Hung Lo [b], Szu-Han Ho [d], Guangrui Xia [e], Osbert Cheng [f], Cheng Tung Huang [f]

[a] Department of Photonics, National Sun Yat-Sen University, Kaohsiung, Taiwan, ROC
[b] Department of Physics, National Sun Yat-Sen University, Kaohsiung, Taiwan, ROC
[c] Center for Nanoscience and Nanotechnology, National Sun Yat-Sen University, Kaohsiung, Taiwan, ROC
[d] Department of Electronics Engineering, National Chiao Tung University, Hsinchu, Taiwan, ROC
[e] Department of Materials Engineering, the University of British Columbia, Vancouver, Canada
[f] Device Department, United Microelectronics Corporation, Tainan Science Park, Taiwan, ROC

ARTICLE INFO

Available online 16 July 2010

Keywords:
SOI
GIFBE
Electron-valance band tunneling
Strained silicon

ABSTRACT

The influence of tensile mechanical strain on gate-induced floating-body effect (GIFBE) in advanced partially depleted SOI n-MOSFETs was investigated. Both drain current and mobility enhance after applying strain due to the reduction of average transfer effective mass. However, it was found that the GIFBE becomes serious under the mechanical strain. To explain this phenomenon, we first clarify the mechanism of GIFBE using different operation conditions. The experiment results indicate that the GIFBE can be attributed to the anode hole injection (AHI) rather than the widely accepted mechanism of electron band (EVB) tunneling. Based on the AHI model, the enhanced GIFBE under the mechanical strain is mainly due to the narrowing of band gap induced by the strain in the poly-gate.

1. Introduction

Silicon-on-insulator (SOI) CMOS devices are attractive since they provide high current drivability and reduced junction capacitance as compared to bulk-Si devices [1]. However, as the gate length scales below the 100 nm, it becomes critical to realize the high drive current due to the degradation of carrier mobility caused by the required increase in channel doping [2]. Therefore, the use of strained silicon technique offers an alternative method to enhance the SOI performance through an increased channel mobility. In addition, with the aggressive shrinking of gate oxide thickness, the strain technique can also reduce the gradually increasing gate tunneling current in advanced SOI devices [3]. According to a previous study, the increasing tunneling current in partially depleted (PD) SOI MOSFETs has been reported to cause a new floating-body effect in the linear operation region, phenomenon referred to as "linear kink effect" (LKE) or "gate-induced floating-body effect" (GIFBE) [4]–[6]. However, the influence of mechanical strain on GIFBE has not been studied yet. Besides, there are few studies that confirm the origin of the GIFBE in PD SOI MOSFETs by using systematical operation conditions. Therefore, the purpose of this work is to clarify the mechanism of GIFBE for PD SOI n-MOSFETs first. Then, based on our new model, we further study the influence of mechanical strain on GIFBE. The experimental results demonstrate that anode hole injection (AHI) from the poly-gate is the main dominant mechanism responsible for GIFBE. Based on the AHI model, it was found that the mechanical strain has a dramatic impact on the GIFBE of PD SOI n-MOSFET.

2. Experiment

Using 65 nm SOI CMOS technology, PD SOI n-type MOSFETs are employed the T-gate structure to investigate the GIFBE mechanism. The SOI wafers were fabricated using SMART-CUT technology. The silicon film and buried oxide thicknesses for the devices are 75 nm and 145 nm, respectively. The gate oxide with a thickness of 12 Å was grown by *in-situ* steam generation (ISSG), with a channel doping concentration of about 3×10^{18} cm^{-3}. The channel currents follow in the <110>direction on (100) substrates. In this work, devices with a channel width (W) of 1 um, and a length (L) ranging from 1 μm to 0.2 μm were selected. The devices with a floating or a grounded body were measured to study the phenomenon of LKE. To further investigate the GIFBE, temperature-dependent electrical characteristics were performed at temperatures ranging from 303 K to 453 K. In order to study the influence of the mechanical strain on GIFBE, the tensile strain along the channel length was introduced by mechanical bending as follows; the thickness of the silicon substrate was reduced from 800 μm to 50 μm using a Struers RotoPol-21 polisher.

* Corresponding author. Department of Physics and Institute of Electro-Optical Engineering, Nation Sun Yat-Sen University, 70 Lien-hai Rd., Kaohsiung 80424, Taiwan, ROC. Tel.: +886 7 5252000x3708; fax: +886 7 5253709.
E-mail address: tcchang@mail.phys.nsysu.edu.tw (T.-C. Chang).

0257-8972/$ – see front matter © 2010 Elsevier B.V. All rights reserved.
doi:10.1016/j.surfcoat.2010.07.028

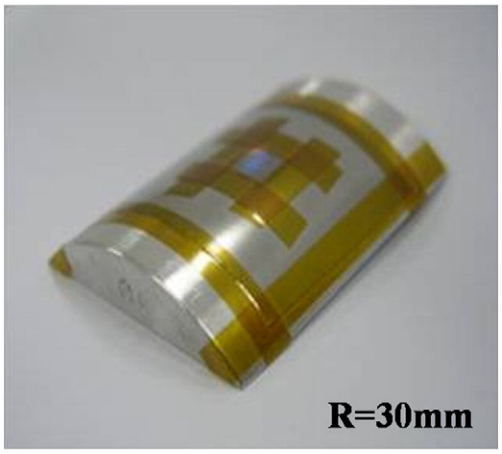

Fig. 1. The illustration of sample bending on the holder with curvature radius R = 30 mm.

Subsequently, the silicon substrate was adhered to a metal foil and then fixed on a bending form, as shown in the Fig. 1. All experimental curves were measured using a Keithley 4200 semiconductor parameter analyzer.

3. Results and discussion

Fig. 2(a) shows the transfer characteristics in the linear region (V_D = 50 mV) for a PD SOI n-type MOSFET under floating-body (FB) and grounded-body (GB) operations. It can be clearly observed that an excess of drain current and a second *gm* peak appear in the FB device. To realize the second peak in this unusual gm–V_G curve, the I_B–V_G transfer characteristic was also measured for comparison. Obviously, the I_B under the GB operation increases rapidly beyond the gate voltage of 0.9 V, corresponding to the second *gm* peak. This phenomenon indicates that additional carriers (hole) accumulate in the body beyond this voltage under the FB operation. Therefore, the body potential increases exponentially, which causes the threshold voltage (V_T) to reduce, resulting in a higher drain current (Id_{lin}) and the second *gm* peak in the linear region.

To examine the origin of additional carriers (hole) caused by the gate leakage current (I_G), Fig. 3(a) illustrates the I_G and I_B versus gate voltage (V_G) for different N^+ poly-gate area (1 μm^2 to 0.2 μm^2) while the source/drain (S/D) is grounded. Clearly, the I_B has a significant enhancement as the I_G increases, meaning that the source of I_B is strongly dependent on the I_G. Furthermore, the linear relationship between I_B and I_G is also obtained as shown in the inset of Fig. 3(a). The I_B–V_G curve in Fig. 3(a) shows that the V_G corresponding to the rapid increase of I_B for different N^+ poly-gate areas always locates around 0.9 V. This indicates that additional carriers only can be generated under certain vertical electrical field regardless of the poly-gate area.

It was proposed that the I_G consists of electron tunneling from the conduction band (ECB), electron tunneling from the valence band (EVB), and hole tunneling from the valence band (HVB) as shown in Fig. 3(b) [7]. In fact, the hole accumulation in the p^- substrate has been explained due to EVB and HVB tunneling currents under a FB condition. However the EVB tunneling model was widely accepted to explain the LKE phenomenon because the HVB is typically very small for NMOS [5].

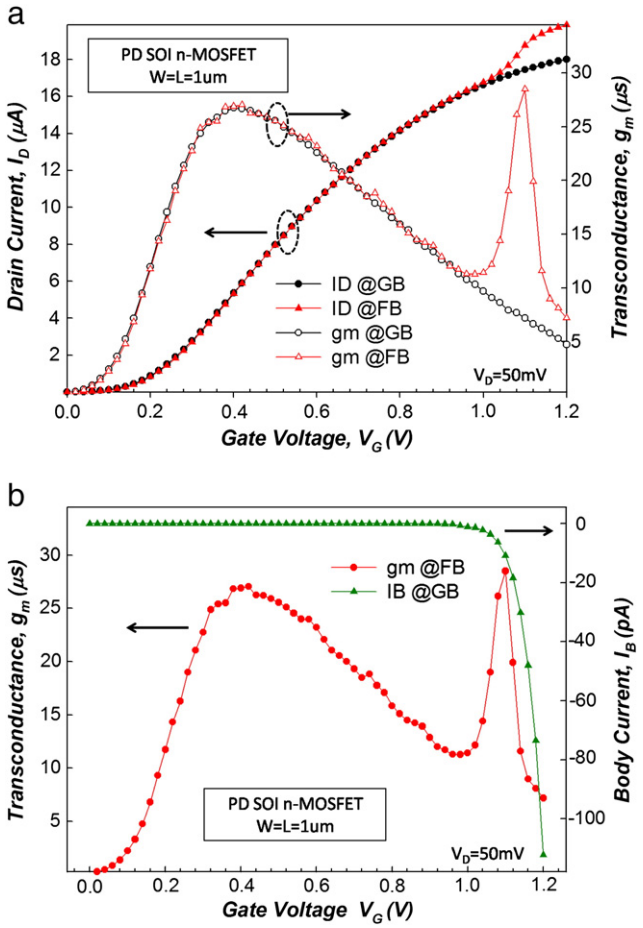

Fig. 2. (a) Transfer characteristics for PD SOI n-MOSFETs under GB and FB operations. (b) The *gm* as a function of the gate voltage under the FB operation in the linear region (V_D = 50 mV). I_B is measured under the GB operation.

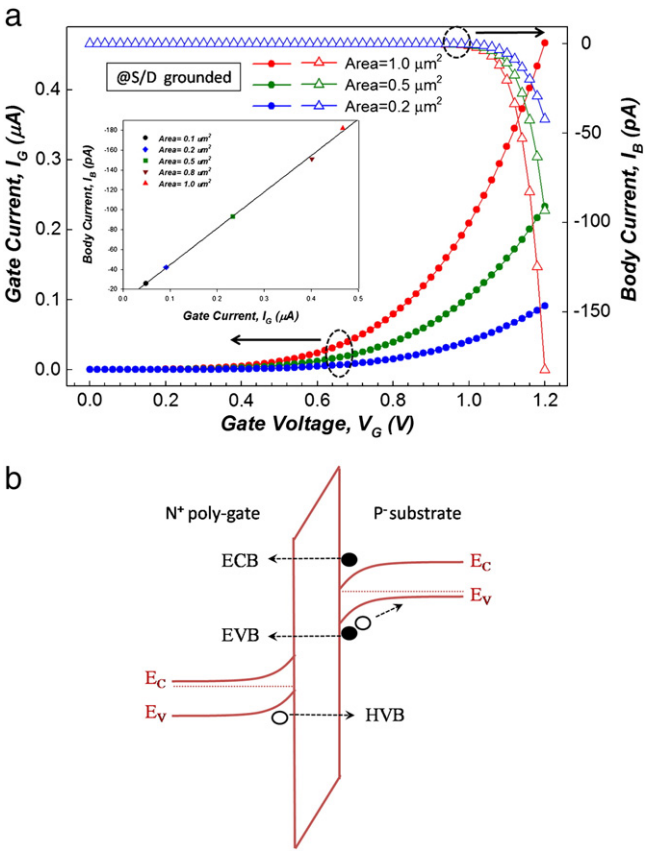

Fig. 3. (a) I_G–V_G and I_B–V_G curves for different N^+ poly-gate areas. Inset displays the linear relationship between I_B and I_G for different N^+ poly-gate areas. (b) The schematic diagram of the different gate tunneling components in an ultra thin gate oxide n-MOSFET.

In Fig. 4(a), the schematic band diagram of EVB shows that the electrons tunnel from the valence band of the Si substrate to the poly-gate conduction band under a sufficiently large vertical electric field. As a result, holes accumulate in the body due to the floating body, which leads to a rise in the body potential. However, the other mechanism, that of AHI [8], also shown in the Fig. 4(a), is also a possible model to explain the LKE. In AHI, when the gate oxide is thin enough, electrons can tunnel from the inversion layer to the poly-gate (anode) and generate hot holes by impact ionization in the poly depletion region. Then these hot holes can inject over or through the anode/oxide interface energy barrier and traverse the oxide layer to the body (cathode). Consequently, the HVB tunneling current becomes significant due to the increase of AHI tunneling current from the poly-gate to the p^- substrate. Both mechanisms generate holes that accumulate in the body, but there are two key differences between the EVB tunneling and AHI model. One is the source of electrons: the electrons in the EVB tunneling model come from the band, but the source of electrons in the AHI model is from the conduction band. The other difference is that the intensity of the vertical electric field in the EVB tunneling model is larger than that in the AHI model. This is because the V_G in the EVB tunneling model needs to be larger than the silicon band gap (1.1 V) to make the band energy level in the silicon substrate align with the gate conduction band [7]. Our experimental results that identify the rapid increase of I_B for different N^+ poly-gate areas located at around 0.9 V imply that the AHI model is more likely to be responsible for the GIFBE.

To further verify that the AHI model is the dominant mechanism of GIFBE, two operation conditions illustrated in Fig. 4(b) are performed to distinguish the different sources of I_G that result in hole accumulation. We measured the I_G and I_B versus V_G of the device under S/D floating and grounded operations. The result under the S/D floating operation is shown in Fig. 5, where it can be clearly observed that the gate leakage current becomes insignificant because the S/D cannot supply sufficient minority carriers (electrons) to the inversion layer. The I_B is not evident (~0.1 pA) in this operation. On the contrary, both currents show very pronounced increases under the S/D grounded operation. The results prove that the origin of GIFBE can be attributed to the electrons in the inversion layer, rather than the electron-hole pair separated in the valence band of the P^- substrate. Therefore, the AHI model is the dominant mechanism responsible for GIFBE.

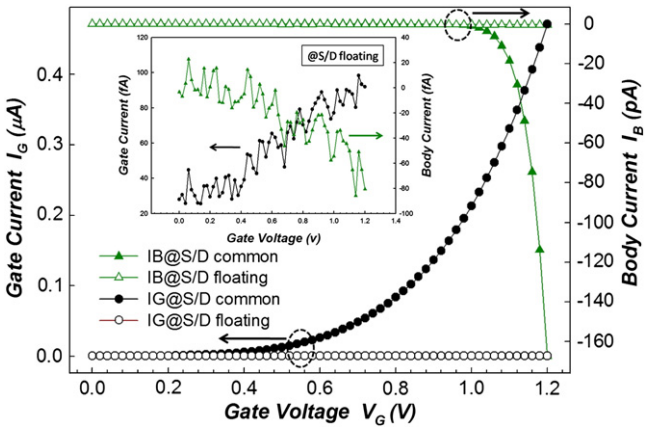

Fig. 5. I_G–V_G and I_B–V_G characteristics for PD SOI n-MOSFET under S/D floating and grounded operations. The inset shows alone the I_G–V_G and I_B–V_G with S/D floating.

The second *gm* peak introduced in Fig. 2 was also analyzed as a function of temperature in the range from 303 K to 453 K. Fig. 6(a) shows that the second peak amplitude becomes smaller and shifts left as the temperature increases. This reduction is ascribed to an increase in recombination rate in the source and drain junctions as temperature increases [9]. To investigate the second *gm* peak shift, the I_B–V_G curve as a function of temperature was also measured and shown in Fig. 6(b) for comparison. It shows that the left shift trend of I_B against temperature is similar to that of the second *gm* peak. However, I_B has no significant change after a V_T correction for different temperatures, as shown in the insert of Fig. 6(b). The results provide further evidence that hole injection from the anode is direct tunneling, because it is independent of temperature.

To further investigate the influence of tensile strain on GIFBE, Fig. 7(a) presents the transfer characteristics of the SOI n-MOSFET under the GB operation with mechanical strain, as compared to the un-strained device (without strain). The result indicates that the Id_{lin} and *gm* improve 3.0% and 3.4%, respectively. The enhancement can be attributed to the reduction in the effective mass and intervalley scattering caused by the tensile strain effect [10]. In addition, the transfer characteristics of the devices under the FB operation both with and without tensile mechanical strain are

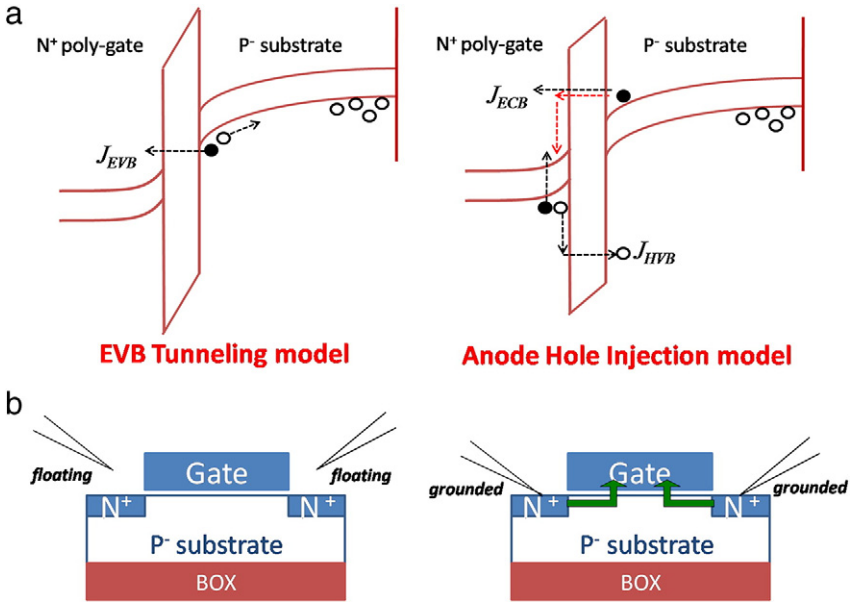

Fig. 4. The schematic diagrams of (a) EVB tunneling and AHI models for an ultra thin gate oxide of PD SOI n-MOSFET and (b) the device under S/D floating and grounded operations.

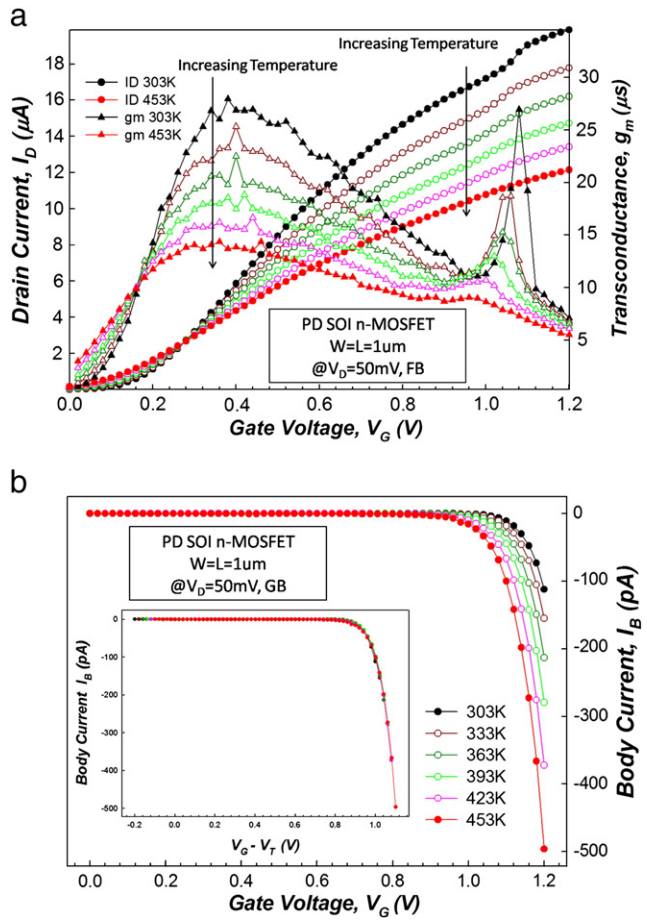

Fig. 6. (a) Transfer characteristics as a function of temperature varying from 303 to 453 K under the FB operation and (b) I_B –V_G characteristics of the PD SOI n-MOSFET with body-contact for different temperatures. The inset shows the I_B –V_G after a V_T correction, where the V_T is obtained from linear extrapolation from the gm_{max}.

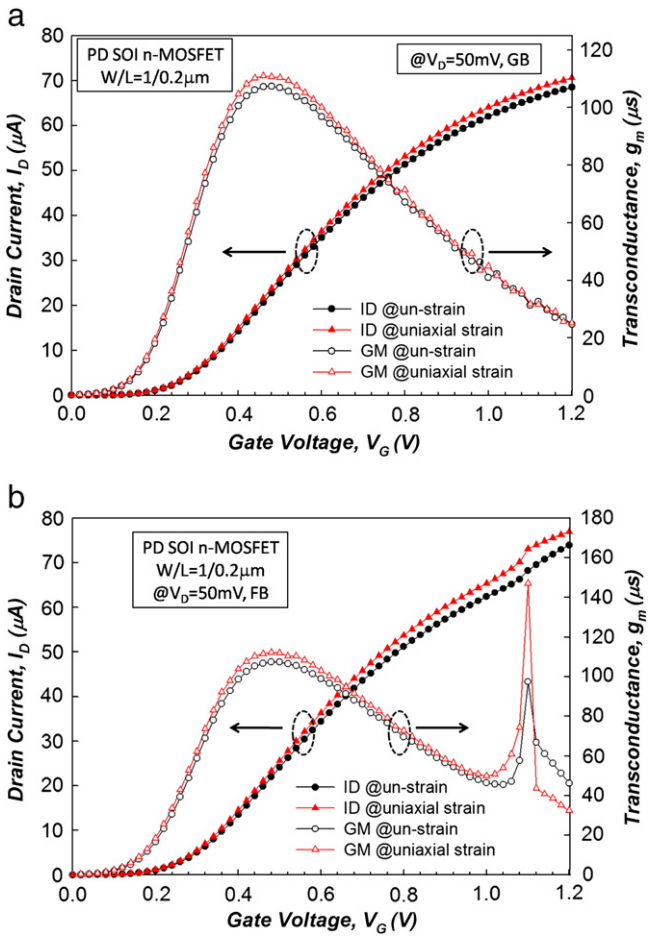

Fig. 7. Transfer characteristics for PD SOI n-MOSFETs with and without mechanical strain under (a) the GB operation and (b) the FB operation.

shown in Fig. 7(b). Under the mechanical strain, the position of GIFBE shifts toward a lower V_G and the magnitude of second *gm* peak increases obviously. Furthermore, after the second peak, the *gm* for the strained device recovers its initial trend (under the GB operation trend), as compared to the un-strained device.

To realize the influence of the strain on the second *gm* peak clearly, the I_G and I_B versus V_G with and without mechanical strain were measured in Fig. 8. It shows that the left shift trend of I_B under mechanical strain is similar to that of the second *gm* peak. Besides, the I_G decreases slightly under the mechanical strain. This opposing reduction is due to the strain-induced change in the conduction band offset between Si and the SiO2 gate dielectric [3].

Based on the AHI model, the I_B generally decreases as the I_G decreases. However, Fig. 8 indicates that even if the I_G decreases under the mechanical strain, the I_B still increases significantly. This unusual result is mainly related to the narrowing band gap induced by the mechanical strain effect [11]–[13]. Because the impact ionization rate is exponential to the energy band gap, the narrowing band gap causes more additional holes to be generated in the poly depletion region, leading to the increase of I_B and a significant second *gm* peak in strained SOI devices. Besides, after the second peak, the *gm* for the strained device recovers its initial trend. This implies that the enhanced I_B causes the body potential to reach the junction diode threshold voltage. Therefore, for the strained device, holes cannot further accumulate in the body, resulting in the *gm* recovery after the second peak [4].

4. Conclusion

In this work, we first demonstrate that the EVB tunneling model is not the dominant mechanism for the GIFBE. When oxide thickness is reduced to only 12 Å, both I_G and I_B are insignificant under the S/D floating operation. Therefore, the GIFBE can be attributed to the electrons of the inversion layer supplied from the S/D. This result indicates that the increase of HVB tunneling current induced by AHI is the dominant mechanism responsible for the GIFBE. By analyzing I_B as a function of

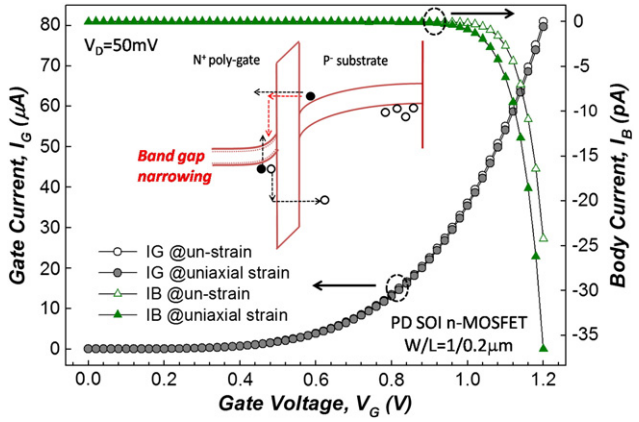

Fig. 8. I_G–V_G and I_B–V_G characteristics for PD SOI n-MOSFET with and without mechanical strain. The inset shows the schematic diagrams of the AHI model under mechanical strain.

temperature, we also prove that the hole current (I_B) is direct tunneling from the poly-gate. This is because I_B is independent of temperature after a V_T correction. Based on the AHI model, it was found that the tensile strain has a strong impact on the GIFBE. This is owing to the band gap narrowing induced by the strain effect in the poly-gate.

Acknowledgments

Part of the work was performed at the United Microelectronics Corporation. The work was supported by the National Science Council under Contract NSC-98-3114-M-110-001, and NSC-97-2112-M-110-009-MY3.

References

[1] J.C. Sturm, K. Tokunaga, J.P. Colinge, IEEE Electron Device Lett. 9 (1988) 460.
[2] T. Ghani, K. Mistry, P. Packan, S. Thompson, Stealer M, Tyagi S, VLSI Tech Dig, 2000 174.
[3] W. Zhao, A. Seabaugh, V. Adams, D. Jovanovic, B. Winstead, IEEE Electron Device Lett. 26 (2005) 410.
[4] A. Mercha, J.M. Rafi, E. Simoen, E. Augendre, C. Claeys, IEEE Trans. Electron Dev. 50 (2003) 1675.
[5] P.G.D. Agopian, J.A. Martino, E. Simoen, C. Claeys, Microelectron 38 (2007) 114.
[6] M. Cassé, J. Pretet, S. Cristoloveanu, T. Poiroux, C. Fenouillet-Beranger, F. Fmleux, C. Raynaud, G. Reimbold, Solid-State Electronics 48 (2004) 1243.
[7] W.-C. Lee, C. Hu, IEEE Trans. Electron Devices 48 (2001) 1366.
[8] K.F. Schuegraf, C. Hu, IEEE Trans. Electron Devices 41 (1994) 761.
[9] L. Vancaillie, V. Kilchytska, P. Delatte, L. Demeus, H. Matsuhashi, F. Ichikawa, D. Flandre, IEEE Int. SOI Conf. (2003) 78.
[10] S.E. Thompson, M. Armstrong, C. Auth, S. Cea, R. Chau, G. Glass, IEEE Electron Device Lett. 25 (2004) 191.
[11] F.A.I.R. RB, J. Appl. Phys. 50 (1979) 860.
[12] T. Irisawa, T. Numata, N. Sugiyama, S. Takagi, IEEE Trans Electron Dev. 52 (2005) 993.
[13] Y.J. Kuo, T.C. Chang, P.H. Yeh, S.C. Chen, C.H. Dai, C.H. Chao, Thin Solid Films 517 (2009) 1715.